

# Color Error from RGB-Stripe Pixel Structure

*M. Kanazawa, K. Hamada and F. Okano*  
*NHK Science & Technical Research Laboratories*  
*Tokyo, Japan*

## Abstract

Most direct-view type color displays have a sub pixel structure such as the RGB-stripe structure. The video data for R and B are produced on condition that they are reproduced at the same position as G but they are displayed on the screen with 1/3 of a pixel separation from the corresponding G pixel. This pixel structure thus entails a convergence error of 1/3 of a pixel. The modified s-CIELAB method was applied to investigate color errors produced by the RGB-stripe pixel structure. The results show that the pixel structure can degrade the image quality even in a viewing distance where the pixel structure is not visible, because the color difference caused by the structure has a low frequency component and the human vision can detect it. The same method was applied to the convergence error and showed that the necessary convergence accuracy is around 1/4 of a pixel.

## Introduction

Most direct-view type color displays have a sub pixel structure such as the RGB-stripe structure. The video data for R and B are produced on condition that they are reproduced at the same position as G but they are displayed on the screen with 1/3 of a pixel separation from the corresponding G pixel. This pixel structure thus entails a convergence error of 1/3 of a pixel. The authors propose the modified s-CIELAB method and apply this method to investigate color errors produced by the RGB-stripe pixel structure. The same method is applied to the convergence error.

## Modified s-CIELAB Method

### False Color Components Due to s-CIELAB

To investigate the color reproduction of images, s-CIELAB has been introduced and accomplished success to some extent.<sup>1</sup> This tool enables color engineers to predict the color reproduction error after signal processing. Figure 1 shows the basic flow chart of the procedure in s-CIELAB. Equation (1) shows the conversion from X,Y,Z to the three components Lum,R/G,B/Y. Their high frequency elements are reduced through different LPF (low pass filter). Let's use a mark <> to represent the output of LPF and the subscripts of <> (L, RG, BY) to represent LPF characteristics.

$$\begin{pmatrix} Lum \\ R/G \\ B/Y \end{pmatrix} = \begin{pmatrix} 0.279 & 0.720 & -0.107 \\ -0.449 & 0.290 & -0.077 \\ 0.086 & -0.590 & 0.501 \end{pmatrix} \begin{pmatrix} X \\ Y \\ Z \end{pmatrix} \quad (1)$$

Though the procedure shown in Fig. 1 looks reasonable, some errors can be introduced by the conversion to X,Y,Z values from the LPF processed components. To explain the cause simply, we describe each component into high frequency element; <><sub>High</sub> and low frequency element; <><sub>Low</sub>. It is clear that the high frequency element is produced from only the Lum component. From re-conversion of equation (1), equation (2) is obtained. The equation (3), with which the color coordinates, xy, is calculated, shows that x, y values can be drifted by unexpected amount due to the high frequency components, because the ratio of both components is different between the numerator and the denominator.

$$\begin{aligned} X &= 0.6266 \cdot \langle Lum \rangle_{HIGH} + \langle X \rangle_{LOW} \\ Y &= 1.3699 \cdot \langle Lum \rangle_{HIGH} + \langle Y \rangle_{LOW} \\ Z &= 1.5057 \cdot \langle Lum \rangle_{HIGH} + \langle Z \rangle_{LOW} \end{aligned} \quad (2)$$

$$\begin{aligned} x &= \frac{0.6266 \cdot \langle Lum \rangle_{HIGH} + \langle X \rangle_{LOW}}{3.5022 \cdot \langle Lum \rangle_{HIGH} + \langle X+Y+Z \rangle_{LOW}} \\ y &= \frac{1.3699 \cdot \langle Lum \rangle_{HIGH} + \langle Y \rangle_{LOW}}{3.5022 \cdot \langle Lum \rangle_{HIGH} + \langle X+Y+Z \rangle_{LOW}} \end{aligned} \quad (3)$$

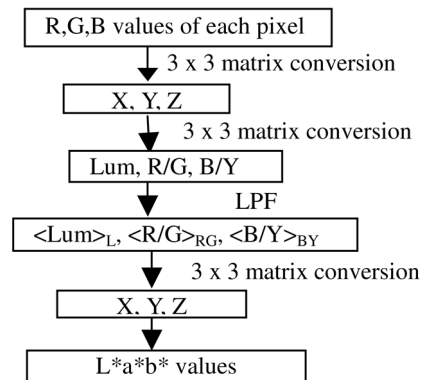


Figure 1. Flow chart for s-CIELAB

In order to evaluate the artifact from different LPFs, the input image is set to a combination of black and white bar patterns, as shown in Fig. 2 in a condition that the widths of white and black bars are 2 and 6 pixels, and one pixel occupies 1/60 degrees of the viewing angle for the viewer. From the Lum, R/G and B/Y components after the LPF processing shown in Fig. 3, CIE x and y coordinates are obtained as shown in Fig. 4. Because the input is achromatic, the change of the x, y coordinates means the false color components. This artifact is caused by a calculation combining components from different LPF.

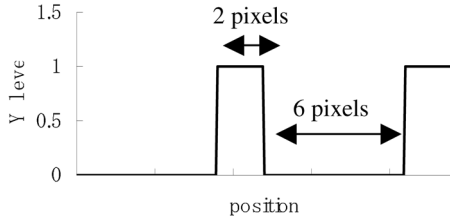


Figure 2. Example of Input pattern

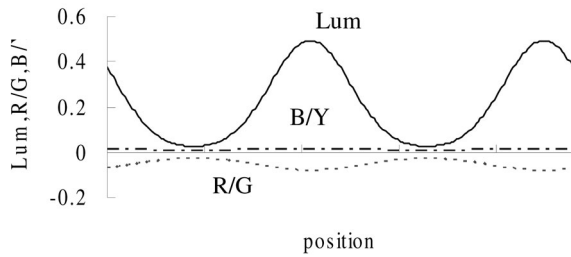


Figure 3. Three components after LPF

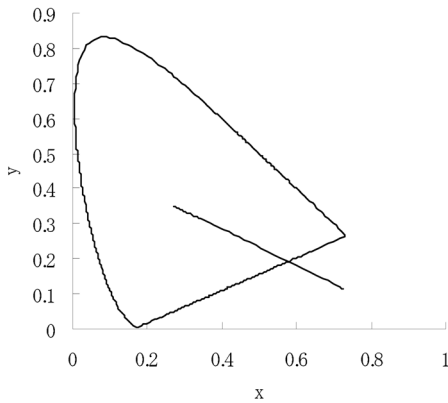


Figure 4. Calculated x, y coordinates

### Modification of s-CIELAB

Figure 5 shows the concept of the modification of s-CIELAB. The occurrence of the false color components is avoided because the three components after LPF processing are converted to psychological values directly without combining components from different LPF. We define psychological values  $(rg)^*$  and  $(by)^*$  in equation (4). In the

equation  $( )_w$  means values for the reference white and constants. Please note that the values Y, and  $(X+15Y+3Z)$  are processed in two different LPF in order to calculate  $(rg)^*$  and  $(by)^*$ , because any combination of values from different LPF must be avoided. From  $(rg)^*$  and  $(by)^*$ , CIE  $u^*$  and  $v^*$ , as well as metric chroma can be calculated by (5). No false color is introduced by this modification and can be applied to high-resolution images.

$$(rg)^* \equiv L^* \langle Y \rangle_{R/G} \left\{ \frac{\langle (R/G) \rangle_{R/G}}{\langle X+15 \cdot Y+3 \cdot Z \rangle_{R/G}} - \frac{\langle (R/G) \rangle_w}{\langle X+15 \cdot Y+3 \cdot Z \rangle_w} \right\} \quad (4)$$

$$(by)^* \equiv L^* \langle Y \rangle_{B/Y} \left\{ \frac{\langle (B/Y) \rangle_{B/Y}}{\langle X+15 \cdot Y+3 \cdot Z \rangle_{B/Y}} - \frac{\langle (B/Y) \rangle_w}{\langle X+15 \cdot Y+3 \cdot Z \rangle_w} \right\}$$

$$\begin{pmatrix} (rg)^* \\ (by)^* \end{pmatrix} = \begin{pmatrix} \frac{1.27}{156} & \frac{0.675}{117} \\ \frac{0.243}{156} & \frac{3.095}{117} \end{pmatrix} \cdot \begin{pmatrix} u^* \\ v^* \end{pmatrix} \quad (5)$$

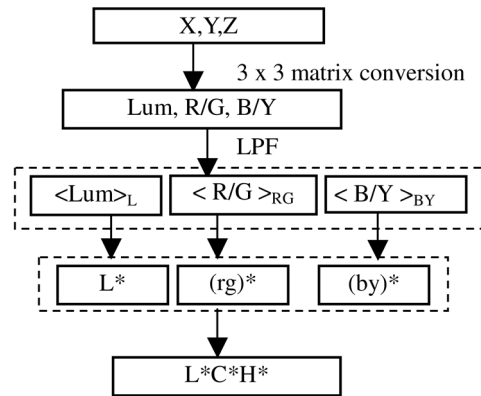


Figure 5. Concept of the flowchart for modified s-CIELAB

## Color Error by the RGB-Stripe Pixel Structure

### Artifact By Pixel Structure

In most direct-view type displays, a pixel structure such as the RGB stripe allows the presentation of color images. The video data for R and B are produced on condition that they are reproduced at the same position as G but they are displayed on the screen with 1/3 of a pixel separation from the corresponding G pixel (Fig. 6). This pixel structure thus entails a convergence error of 1/3 of a pixel. Although the pixel structure is invisible under typical viewing conditions, it is possible for viewers to notice the color errors, which are caused by this structure. On the other hand, in the case of typical CRT displays, the video signals are sent in the analog format and the color error will not be seen in the same viewing condition. This is because the R and B sub pixels are driven by interpolated signals corresponding to their positions and there is no geometrical difference between the positions of the sub pixels and the driving

video signals. Therefore, the above color error can happen on flat panel displays with a digital signal input.

Denoting the input signal as  $f(x)$  (achromatic), any color component can be expressed by (6). When  $f(x)$  is a sinusoidal wave of frequency  $\omega_0$ , the Fourier transform is calculated as (7).

$$f_R(x) + f_G(x) + f_B(x) \quad (6)$$

where

$$f_R(x) = C_1 \cdot f(n \cdot \Delta x) \cdot \sum_{n=-\infty}^{\infty} \left\{ h\left(x - n \cdot \Delta x + \frac{\Delta x}{2}\right) - h\left(x - n \cdot \Delta x + \frac{\Delta x}{6}\right) \right\}$$

$$f_G(x) = C_2 \cdot f(n \cdot \Delta x) \cdot \sum_{n=-\infty}^{\infty} \left\{ h\left(x - n \cdot \Delta x + \frac{\Delta x}{6}\right) - h\left(x - n \cdot \Delta x + \frac{\Delta x}{6}\right) \right\}$$

$$f_B(x) = C_3 \cdot f(n \cdot \Delta x) \cdot \sum_{n=-\infty}^{\infty} \left\{ h\left(x - n \cdot \Delta x + \frac{\Delta x}{6}\right) - h\left(x - n \cdot \Delta x + \frac{\Delta x}{2}\right) \right\}$$

$$h(x) = \begin{cases} 1, & x \geq 0 \\ 0, & x < 0 \end{cases}$$

$$F(\omega_0) = \frac{2}{\omega} \cdot \sin\left(\frac{\omega \cdot \Delta x}{6}\right) \cdot \left\{ C_1 \cdot e^{-i \frac{\omega \Delta x}{3}} + C_2 + C_3 \cdot e^{-i \frac{\omega \Delta x}{3}} \right\} \quad (7)$$

Image capturing

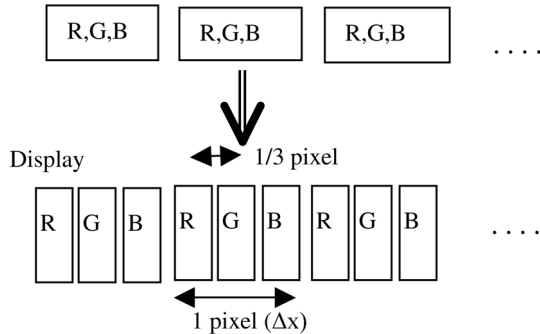


Figure 6. Image capturing and RGB stripe structure

Figure 7 shows an example of Fourier transform for the (B/Y) component of s-CIELAB. It is shown that even with an achromatic input signal, color components are introduced due to the pixel structure.

**Calculation of Color Error**

The modified s-CIELAB method is applied to evaluate the subjective magnitude of the artificial color component described in the previous chapter. The image to be evaluated is a black line in the white field, viewed from a distance where 1.0 degree corresponds to 60 pixels. Figure 8 shows the human visual characteristics on this viewing condition based on sCIELAB and the Fourier components of Fig. 7. Under this condition, the pixel structure (30 cycles/deg.) is invisible, because the response is nearly 0.0 for all of the s-CIELAB components, but the color difference component is visible. The metric chroma is

calculated as the subjective magnitude of the color component. Figures 9 and 10 show the results for a one-pixel-wide and a ten-pixel-wide black line, respectively. The abscissa represents position within the image and the RGB stripes for the white area are also shown where the area without any RGB values corresponds to the black lines. As is shown in the figures, there are two peaks in the distribution of the metric chroma, and because the order of the sub-pixels is R, G, and B, the left-hand peak indicates a bluish area and the right indicates a reddish area. The results show that the color component will not be visible with a narrow black line but will be visible with a wide line.

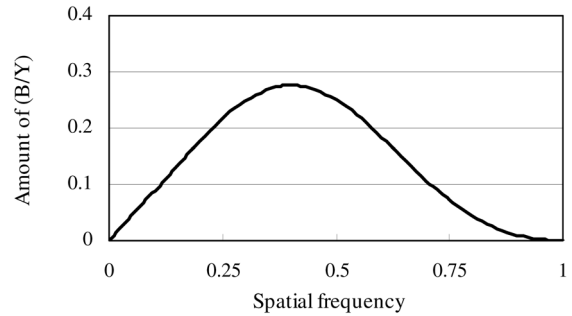


Figure 7. Fourier transform of (B/Y) due to pixel structure

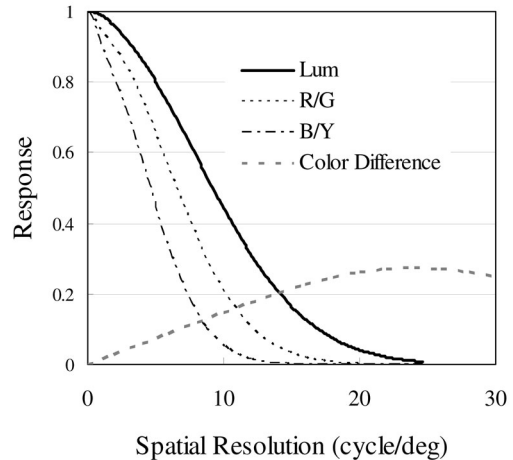


Figure 8. Human visual characteristics

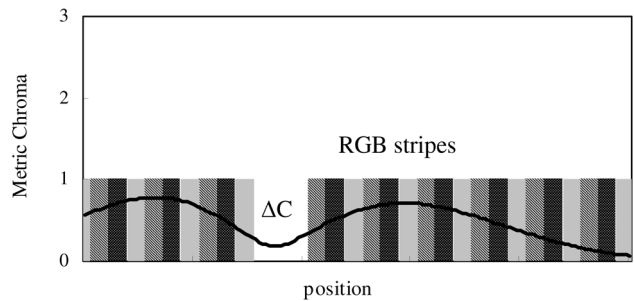


Figure 9. Metric chroma for a one-pixel-wide black line

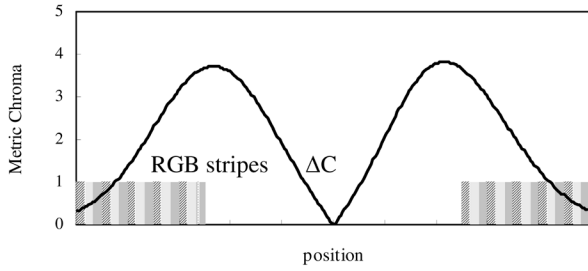


Figure 10. Metric chroma for a ten-pixel-wide black line

This can be explained by Fig. 11 and Fig. 12, which show the psychological values  $(rg)^*$  and  $(by)^*$  in equation (4) for black area after white and white area after black. These values are opposite because the verge portion is blue in Fig. 11 and red in Fig. 12. Therefore, when a stripe is narrow, these values cancel each other. Figure 13 shows the relationship between the maximum value of the metric chroma and the width of the black line. The figure indicates that the color component will be visible in a monochromatic image with a black line that is wider than 4 pixels, because the magnitude of the metric chroma is greater than 3.0 for lines in that range. It should be reminded that the visibility of the color component depends on the viewing distance. The results show the pixel structure can degrade the image quality even in a viewing distance where the pixel structure is not visible, because human vision can detect the disparity between the RGB stripe's positions in that condition. This color error may be disturbing to CAD users when drawings are displayed on flat-panel displays, such as LCDs. This is particularly so for wide vertical lines.

The effect described in this chapter can be seen easily. By making RGB stripes on a paper with a color printer, false color would be observed by covering some of the paper with a black bar.

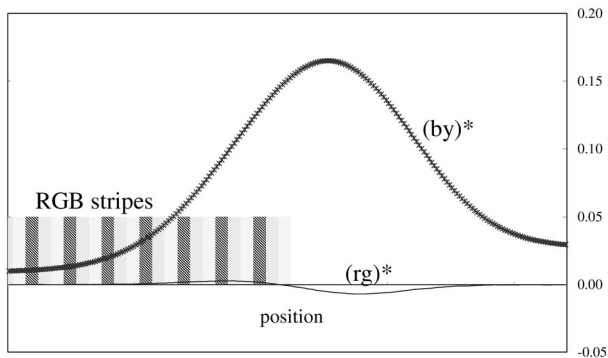


Figure 11.  $(rg)^*$  and  $(by)^*$  for black area after white

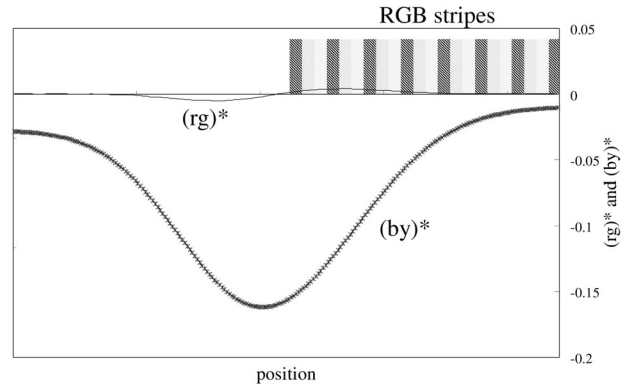


Figure 12.  $(rg)^*$  and  $(by)^*$  for white area after black

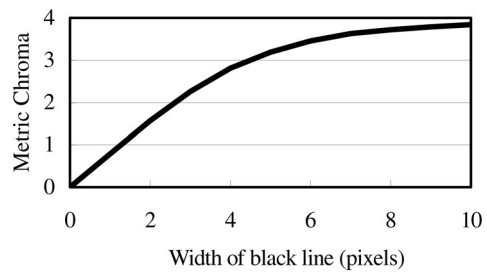


Figure 13. Maximum of the metric chroma for black lines of varied width

### Improvement of Color Error

A simple signal processing can reduce the color error described above. Figure 14 shows the basic flowchart of the signal processing. The video signals for R and B are interpolated with neighboring pixel's signals, while that for G is delayed. With this processing, the psychological values  $(rg)^*$  and  $(by)^*$  of Fig. 11 and Fig. 12 are reduced to less than 0.1 times, as shown in Fig. 15 and Fig. 16.

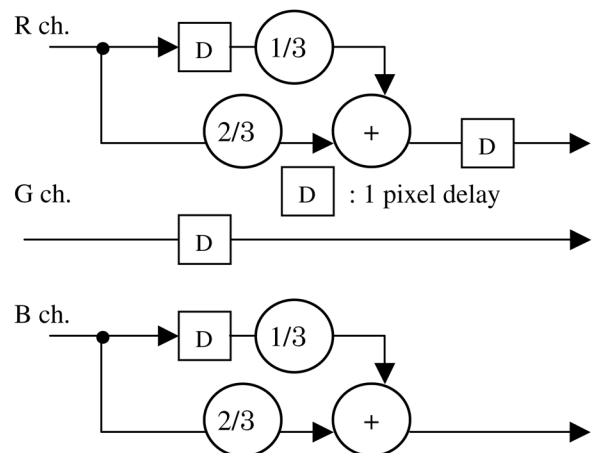


Figure 14. Signal processing to reduce the color error

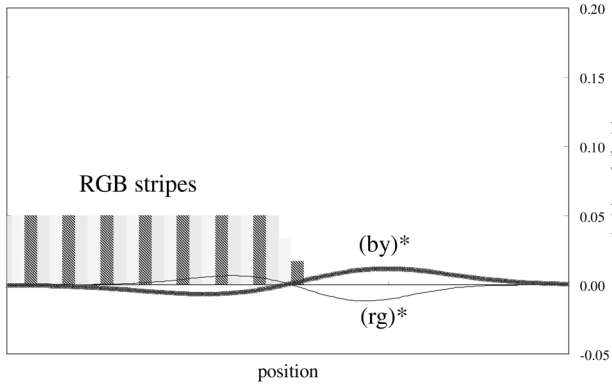


Figure 15.  $(rg)^*$  and  $(by)^*$  for black area after white after the signal processing

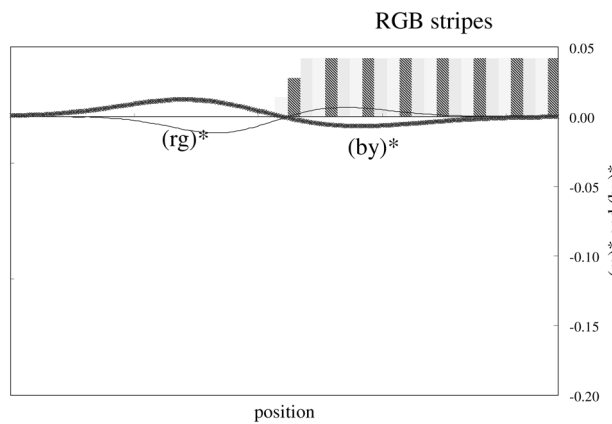


Figure 16.  $(rg)^*$  and  $(by)^*$  for white area after black after the signal processing

### Convergence Error

The same procedure is applied to the evaluation of convergence error. The input image is a monochromatic sinusoidal signal and the viewing distance is the same as for the above calculation. Figure 17 shows the results. The metric chroma is calculated for the convergence error of red, where the amount of error is 1/8, 1/4, 3/8, 1/2, 2/3 and 1 pixel width.

It is shown that a convergence error of more than 1/4 pixels would be detectable. Therefore, the accuracy of the convergence adjustment is desired to be less than 1/4 pixels in order to avoid the degradation on the color reproduction. It is also shown that reproduction of the frequency range around 0.2 times the Nyquist frequency is very sensitive to the convergence error.

A simple simulation was carried out with a 10.4-inch XGA LCD display. The author observed black stripes of various widths with a convergence error of one pixel for red from 90 cm away from the screen. Figure 18 shows the results with calculated metric chroma values. The result is similar to the discussion in Fig. 13.

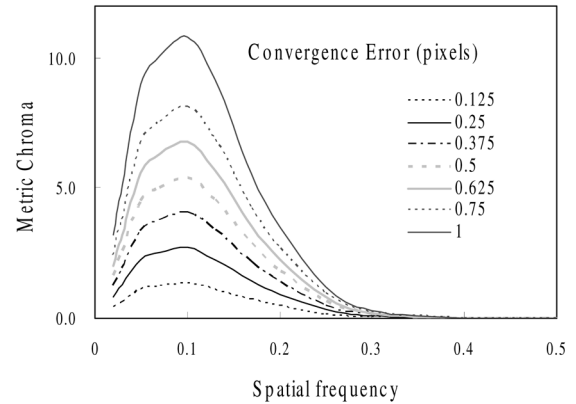


Figure 17. Metric chroma due to convergence error

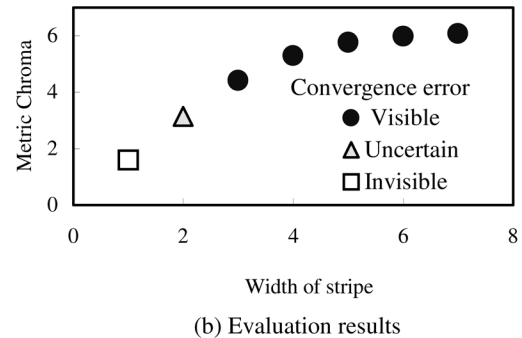
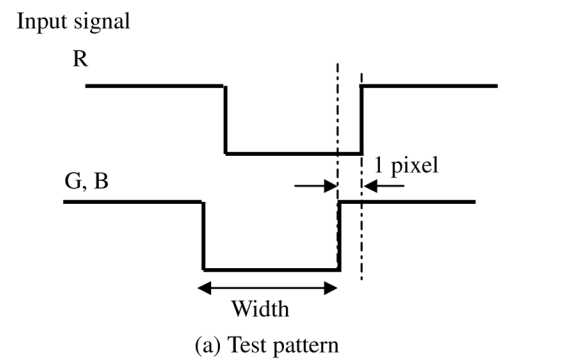


Figure 18. Metric chroma for one pixel convergence error and evaluation result

### Conclusion

A modified sCIELAB method was used to evaluate the draw-backs of the RGB-stripe structure in direct-view type displays. This showed that there would be visible color components in monochromatic images that include a relatively wide black line on a white background. These color components can be seen easily with color stripes and black bars using a color printer. The result means that the pixel structure can affect the human vision and degrade the image quality even in a viewing distance where the pixel structure is not visible. It is also shown that a simple signal processing can reduce these color components effectively.

The procedure can be adapted to any pixel structures other than the RGB stripe.

The modified sCIELAB method was also applied to evaluate the effect of convergence error. This showed that a convergence error of more than 1/4 pixels produces a visible color and that reproduction of the frequency range around 0.2 times the Nyquist frequency is very sensitive to the convergence error.

### References

1. X. Zhang et al; "A spatial extension of CIELAB for digital color-image reproduction" *Journal of the SID*, 5/1, 1997 pp.61~63
2. M. Kanazawa, et al; "A proposal of modification for s-CIELAB", under review for the *Journal of the SID*

### Biography

**Masaru Kanazawa** received his MS degree in electronics from the Graduate School of Hokkaido University in 1979. Since then, he has been working for the Japan Broadcasting Corporation (NHK). He is currently a senior research engineer at the NHK Science and Technical Research Laboratories and is engaged in the development of ultra-

high-definition video systems. Mr. Kanazawa is a member of the Institute of Electronics, Information and Communication Engineers (EIC), the Institute of Image Information and Television Engineers of Japan (ITE), and SID.

**Kouichi Hamada** received his MS degree from the Graduate School of University of Tokyo in 1996. Since then, he has been working for the NHK Science and Technical Labs. He is working in the fields of video signal digital coding, display systems and the driving of plasma displays, and ultra wide-screen & high definition video systems. Mr. Hamada is a member of the Institute of Image Information and Television Engineers of Japan (ITE).

**Fumio Okano** received his BS, MS, and Ph.D degrees, all in electrical engineering, from Tohoku University, Sendai, Japan, in 1976, 1978, and 1996, respectively. He joined the Japan Broadcasting Corporation (NHK) in 1978. Since 1981, he has been engaged in research into high-definition television (HDTV) cameras, HDTV systems, and 3-D television at the NHK Science and Technical Research Laboratories. Dr. Okano is a member of the Institute of Image Information and Television Engineers of Japan (ITE), OSA, and SPIE, and is a senior member of IEEE.